이학석사 학위논문

HR+ 유방암 내의 단핵구와 대식세포에서의 *SPP1* 발현과 종양침윤림프구의 관련성

SPP1 expression of monocytes and macrophages in HR+ breast cancer is associated with tumour-infiltrating lymphocytes

울 산 대 학 교 대 학 원
의 과 학 과
차 수 민

SPP1 expression of monocytes and macrophages in HR+ breast cancer is associated with tumour-infiltrating lymphocytes

지 도 교 수 이 희 진

이 논문을 이학 석사학위 논문으로 제출함

2024 년 8 월

울 산 대 학 교 대 학 원
의 과 학 과
차 수 민

차수민의 이학석사학위 논문을 인준함

심 사 위 원　　공 경 엽　(인)
심 사 위 원　　이 희 진　(인)
심 사 위 원　　정 병 관　(인)

울 산 대 학 교　대 학 원
2024 년 8 월

Abstract

Breast cancer is a globally prevalent cancer, categorised into hormone receptor-positive (HR+), HER2-positive (HER2+), and triple-negative (TNBC) subtypes. The level of tumour-infiltrating lymphocytes (TILs) is an important prognostic indicator of breast cancer. To explore the divergent roles of TIL levels across various subtypes and examine their effect on immune cell composition and tumour microenvironment, we employed single-cell RNA sequencing on 31 patients with breast cancer exhibiting different TIL levels and subtypes. We observed elevated SPP1+ macrophages and reduced mucosal-associated invariant T cells in HR+ breast cancer with high TIL levels (TIL high HR+ breast cancer). Furthermore, *SPP1* expression was increased in other monocytes and macrophages (mono/macro) subgroups in TIL high HR+ breast cancer. Both SPP1+ macrophages and TIL high HR+ breast cancer mono/macro showed increased expression of genes related to ECM remodeling. Moreover, cell-cell interaction analyses revealed enhanced SPP1 signalling in the interaction between mono/macro and T cells in TIL high HR+ breast cancer compared to TIL low group. Spatial transcriptomics data of HR+ breast cancer highlighted close proximity of mono/macro, CD8+ T cells, and CD4+ T cells in TIL high HR+ breast cancer compared to TIL low group. Collectively, we discovered a novel role of *SPP1*-expressing mono/macro in influencing T cells within the tumour microenvironment of TIL high HR+ breast cancer. Our findings may explain poor prognosis of HR+ breast cancer associated with elevated TIL levels, suggesting that SPP1+ macrophages could be potentially targeted to improve their prognosis.

Keywords: Breast cancer, Hormone receptor (HR), Tumour-infiltrating lymphocytes, Tumour-associated macrophages, Secreted Phosphoprotein 1

CONTENTS

Introduction

Breast cancer is the second most prevalent type of cancer globally, with an age-standardized incidence rate of 46.8 per 100,000 people in 2022 [1]. It can be classified into three subtypes based on the expression of hormone receptors and HER2 receptor: hormone receptor-positive (HR+), HER2-positive (HER2+) and triple negative breast cancer (TNBC) [2]. A critical prognostic factor in breast cancer is the level of tumour-infiltrating lymphocytes (TILs), which can be assessed via histologic examination [3]. TILs are defined as mononuclear cells, including plasma cells, that infiltrate the stromal tissue within the invasive tumour area [4]. TILs exhibit subtype-specific characteristics, with HER2+ breast cancer and TNBC typically manifest higher TIL levels than HR+ breast cancer [5]. In HER2+ breast cancer and TNBC, increased TIL levels are associated with improved pathological complete response (pCR) rates after neoadjuvant chemotherapy (NAC), longer disease-free survival, and overall survival [6]. Conversely, in HR+ breast cancer, higher TIL levels are linked to shorter overall survival [7, 8].

Numerous immune cell types can modulate TIL function within the tumour microenvironment (TME) [9]. Among these, tumour-associated macrophages (TAMs) represent a significant proportion of breast cancer immune cells and are closely related to unfavourable prognosis [10, 11]. Single-cell RNA sequencing (scRNA-seq) studies have revealed specific TAM subsets linked to T cell infiltration and immunosuppression in patients with breast cancer [12, 13]. However, our knowledge of differences in immune cell composition, including TAMs, between low and high TIL cases is limited, and the influence of such differences on immune cell infiltration remains poorly understood.

Different subtypes of breast cancers have different TMEs [14]. HR+ breast cancer often exhibits not only a low infiltration of TILs but also higher number of TAMs, which are typically immune-suppressive and associated with poor survival [15]. The emergence of novel technologies, including single cell and spatial transcriptomics, has enabled more detailed characterization of the differences in TME among breast cancer subtypes.

Here, we stratified patients with breast cancer based on their TIL levels (‘TIL high’ and ‘TIL low’), considering each subtype (HR+, HER2+, and TNBC). We then analysed the differences in the composition of CD45+ immune cell subtypes using scRNA-seq. Furthermore, we elucidated the

differences in immune cell interactions within the TME between TIL high and TIL low breast cancers, employing cell-cell interaction analysis and spatial transcriptomics.

Materials and methods

Ethics

This study received approval from the Institutional Review Board of Asan Medical Center (2016-0935) and adhered to the principles of the Declaration of Helsinki of 1975, as revised in 1983. All patients provided written informed consent.

Single cell dissociation

Breast cancer tissue was placed in RPMI 1640 medium (11875093, Thermo Fisher Scientific, Waltham, MA, USA) and promptly transported to the laboratory within two hours post-resection. After washing with Dulbecco's Phosphate Buffered Saline (DPBS, L0615, Biowest, Nuaillé, France) containing 1× ZellShield anticontaminant agent (Minerva Biolabs, Berlin, Germany), the tumour tissues were minced into 1-mm-diameter pieces. The minced breast cancer tissue was incubated for 1 h in digestion buffer (DMEM-F12 (11330032, Thermo Fisher Scientific), 2% FBS (Corning, VA, USA), 1% penicillin/streptomycin (15140-122, Thermo Fisher Scientific), 10 μg/mL insulin (51500056, Thermo Fisher Scientific), and 10 ng/mL epidermal growth factor (PHG0311, Thermo Fisher Scientific) supplemented with 1× collagenase/ hyaluronidase (CA094-002, Gendepot, Barker, TX, USA). The digested samples were centrifuged at 80 × g for 30 s, and the resultant supernatant was filtered through a 70-μm nylon mesh strainer (352350, Corning Life Sciences, Tewksbury, MA, USA). The pellet from the digested samples was resuspended in 0.25% trypsin/EDTA (25200072, Thermo Fisher Scientific) and incubated for 3–5 min to release single cells. Once a single cell suspension was obtained, cold Hank's balanced salt solution (L0612, Biowest) containing 2% FBS was added, and cells were recovered by centrifugation at 300 × g for 5 min. Subsequently, the cells from the supernatants and the single cells from the pellet were combined, counted, and cryopreserved.

CD45+ cell isolation

CD45+ cells were isolated either by magnetic bead sorting or by fluorescence-activated cell sorting (FACS) sorting. In the magnetic separation method, dead cells were initially removed using a dead cell removal kit (130-090-101, Miltenyi Biotec, Auburn, CA, USA), followed by cell labelling with CD45-microbeads (130-045-801, Miltenyi Biotec) and enriched using a magnetic-activated cell sorting (MACS) column (130-042-901, Miltenyi Biotec) and MACS separator (130-091-051, Miltenyi Biotec). For FACS sorting, single cells were stained with an anti-human CD45 antibody (304016, Biolegend, San Diego, CA, USA) and resuspended in 4',6-diamidino-2-phenylindole solution (D1306, Thermo Fisher Scientific). CD45+ live cells were sorted using FACSAria (BD bioscience, San Jose, CA, USA). The isolated cells were resuspended in CS10 freezing media (100-1061, Stemcell Technologies, Bothell, WA, USA) and stored in an NL2 tank until the next use or were immediately sequenced.

scRNA-seq library preparation and sequencing

scRNA-seq library preparation was carried out using the Chromium Single Cell 3′ Kit v2 and the Chromium Next GEM Single Cell 3′ Kit v3 platform (10x Genomics, Pleasanton, CA, USA). Cell suspension volumes were determined to attain a target capture of either 5,000 or 10,000 cells per sample. This process involved the generation of gel beads in emulsion (GEMs), barcoding, GEM-reverse transcription (RT) clean-up, complementary DNA amplification, and library construction, following the manufacturer's specified protocol. Library quality assessment was then performed using Bioanalyzer 2100 (Agilent, Santa Clara, CA, USA). Subsequently, sequencing was executed using the NovaSeq 6000 System (Illumina, Inc., San Diego, CA, USA), generating 150 base pairs (bp) paired-end reads.

scRNA-seq data processing

To increase the sample size and analyze independent datasets, we performed joint analysis of our dataset with a public dataset (GSA, HRA000477 [16]), which was a single cell RNA sequencing dataset where

TIL values were measured and human CD45+ cells were sorted from breast cancer tissue. Analysis was conducted starting from the Cell Ranger processing stage with raw fastq files. The 10x Genomics Cell Ranger 6.1.2 [17] was used for mapping sequencing reads against the GRCh38 human reference (2020-A, GENCODE v32/Ensembl 98), unique molecular identifier (UMI) counting, and cell identification. Pre-processing using the Seurat package (version 4.1.1) [18] was performed in R (version 4.1.3) [19]. In total, 31 samples were merged. Cells that had >20% mitochondrial genes or unique feature counts over 6,000 or less than 200 were excluded, then 110,059 cells remained. To normalise the dataset, we employed the “NormalizeData” procedure. Scaling was applied to the dataset with 2000 features selected through “FindVariableFeatures”. We then performed principal components analysis (PCA) on the scaled data using “RunPCA” (dims = 1:30). Harmony (version 0.1.0) [20] was employed for batch effect correction, using each sample as a batch assignment. Harmony embedding was used in downstream analysis. Uniform manifold approximation and projection (UMAP) was performed using “RunUMAP”.

Cell type annotation

Azimuth package (version 0.4.5) [18, 21] (reference = PBMC) was used for cell type annotation for CD45+ immune cells. The metadata column named 'predicted.celltype.l2' determined by Azimuth was utilised to isolate immune cells into four groups: T-cell (predicted.celltype.l2 = "CD4 CTL", "CD4 Naive", "CD4 Proliferating", "CD4 TCM", "CD4 TEM", "CD8 Naive", "CD8 Proliferating", "CD8 TCM", "CD8 TEM", "dnT", "gdT", "MAIT", "NK", "NK Proliferating", "NK_CD56bright", and "Treg"), B-cell (predicted.celltype.l2 = "B memory", "B intermediate", "B naive", and "Plasmablast"), DC (predicted.celltype.l2 = "ASDC", "cDC1", "cDC2", and "pDC"), and mono/macro (predicted.celltype.l2 = "CD14 Mono" and "CD16 Mono"). Further annotation was conducted for T cells and mono/macro. Memory T cells (predicted.celltype.l2 = "CD8 TCM”, "CD8 TEM”, "CD4 TCM”, and "CD4 TEM”) were defined based on marker expression. *CCR7* and *SELL* double positive cells (UMI count >0) were annotated as TCM, while others as TEM. Mono/macro cells (predicted.celltype.l2 = "CD14 Mono” and "CD16 Mono”) were separated and clustered (resolution

0.3). Each cluster were named based on expressed marker except mitochondrial genes. Expressed markers were identified using the “FindAllMarkers” function in Seurat with the parameter “pct = 0.5”. Following cell type annotation, each breast cancer subtype was individually analysed in downstream.

Pathway enrichment analysis

Differentially expressed genes (DEGs) were computed for each group using the “FindMarkers” function in Seurat. Specifically, we considered genes as up-regulated if they exhibited an average log2 fold change greater than 1 and a p-value less than 0.05, for further analysis. Pathway enrichment analysis was subsequently conducted using the “enrichPathway” method from the ReactomePA package (version 1.38.0) [22] in R. Bar plots, visualising significant pathways based on an adjusted p-value threshold of less than 0.05 (utilising the Benjamini–Hochberg method), were generated using ggplot2 [23].

Cell-cell interaction analysis

CellChat package (version 1.6.1) [24] was used to analyse cell-to-cell interactions. CellChat object was created using the createCellChat function and CellChatDB human dataset. T cells were categorised into four groups: CD4T ("CD4 CTL", "CD4 Naive", "CD4 Proliferating", "CD4 TCM", and "CD4 TEM"), CD8T ("CD8 Proliferating", "CD8 TCM", "CD8 TEM", and "CD8 Naive"), NK ("NK", "NK Proliferating" and "NK_CD56bright"), and OtherT ("dnT", "gdT", "MAIT", and "Treg"). To identify differential interactions in cell-cell communication and to explore conserved and context-specific signalling pathways across different TIL levels, we compared TIL high and TIL low with “netVisual_diffInteractions” and “rankNet”. Then, we analysed SPP1 signalling in each cell group of varying TIL levels. To visualise SPP1 signalling pathway, “netVisual_heatmap” and “netVisual_aggregate” were used. Identification of signalling roles of cell group was performed by utilising functions “netAnalysis_computeCentrality” and “netAnalysis_signallingRole_network”. To

compute the contribution of each ligand-receptor pair and plot signalling gene expression distribution, “netAnalysis_contribution” and “plotGeneExpression” were employed.

Spatial transcriptomics data processing and signature scoring

Seurat objects for each sample were created using the filtered count matrix and spatial data from the Zenodo data repository [25] via Seurat package. To normalise each sample, we employed the “SCTransform” function. TIL levels of each sample in H&E images were assessed by a certified pathologist.

To identify cell type signatures, markers for each cell group were analysed in scRNA-seq data using the “FindMarkers” function with default parameters. We selected the top 25 markers as signature genes. Signature scoring was conducted through the “AddModuleScore” method with a list of signature genes. To minimize the influence of variations in TIL quantity on the scores, we normalized each score. We scaled and centred the signature scores in R and subsequently employed them for correlation coefficient analysis.

Cell cycle scoring

To assign cell cycle scores to each cell, we utilised G2/M and S phase markers. This calculation was performed using the “CellCycleScoring” function available in the Seurat.

Statistical analysis

The Wilcoxon rank sum test and Kruskal–Wallis rank sum test were performed using R stats package (ver.3.6.2) [19]. Additionally, Spearman’s rank correlation coefficient was calculated using R package ggpubr (ver.0.6.0) [26].

Data availability

The study's datasets are available from the corresponding author upon a reasonable request. The public data used in the research has been specified in the main manuscript.

Results

Heterogeneity of tumor microenvironment in breast cancer

To identify the characteristics of TME in breast cancer and its differences based on TIL levels, we conducted scRNA-seq using isolated CD45+ cells from 21 primary tumour tissues with accompanying TIL data. These TIL levels were evaluated by a certified pathologist using H&E stained slides. We also included 10 samples from the Genome Sequence Archive (GSA, HRA000477) dataset [16]. In total, we analysed 31 samples (21 samples from this study, 10 from GSA database) using scRNA-seq, comprising 16 TNBC (10 and 6) and 11 HR+ (8 and 3) and 4 HER2+ samples (3 and 1). Samples with TIL value ≥10 were classified as TIL high group (n = 18, (TNBC n = 10, HR+ n = 5, and HER2+ n = 3)) and those with <10 as TIL low group (n = 13, (TNBC n = 6, HR+ n = 6, and HER2+ n = 1)) (Table S1). Quality control was carried out to remove low-quality cells, and 110,059 cells were left for analysis (Figure S1a-c). After removing the batch effect, cells were distributed evenly unaffected by sample type, breast cancer subtype, or TIL levels (Figure 1a, b). We clustered and visualised the cells using UMAP (Figure 1c). The annotation was validated using canonical markers (Figure 1e). We performed more detailed annotation of immune cell subtypes with canonical markers and gene signatures (Figure 1d and S1d–h). To investigate a difference in proportion of cell types between samples, we generated plots depicting the proportion of cell type relative to TIL levels and subtypes (Figure 1f, g). Regardless of TIL levels and subtypes, breast cancer showed a high degree of heterogeneity in the proportion of immune cell subtypes (Figure 1g). The proportions of immune cell subtypes did not significantly differ among HR+, HER2+, and TNBC (Figure 1h).

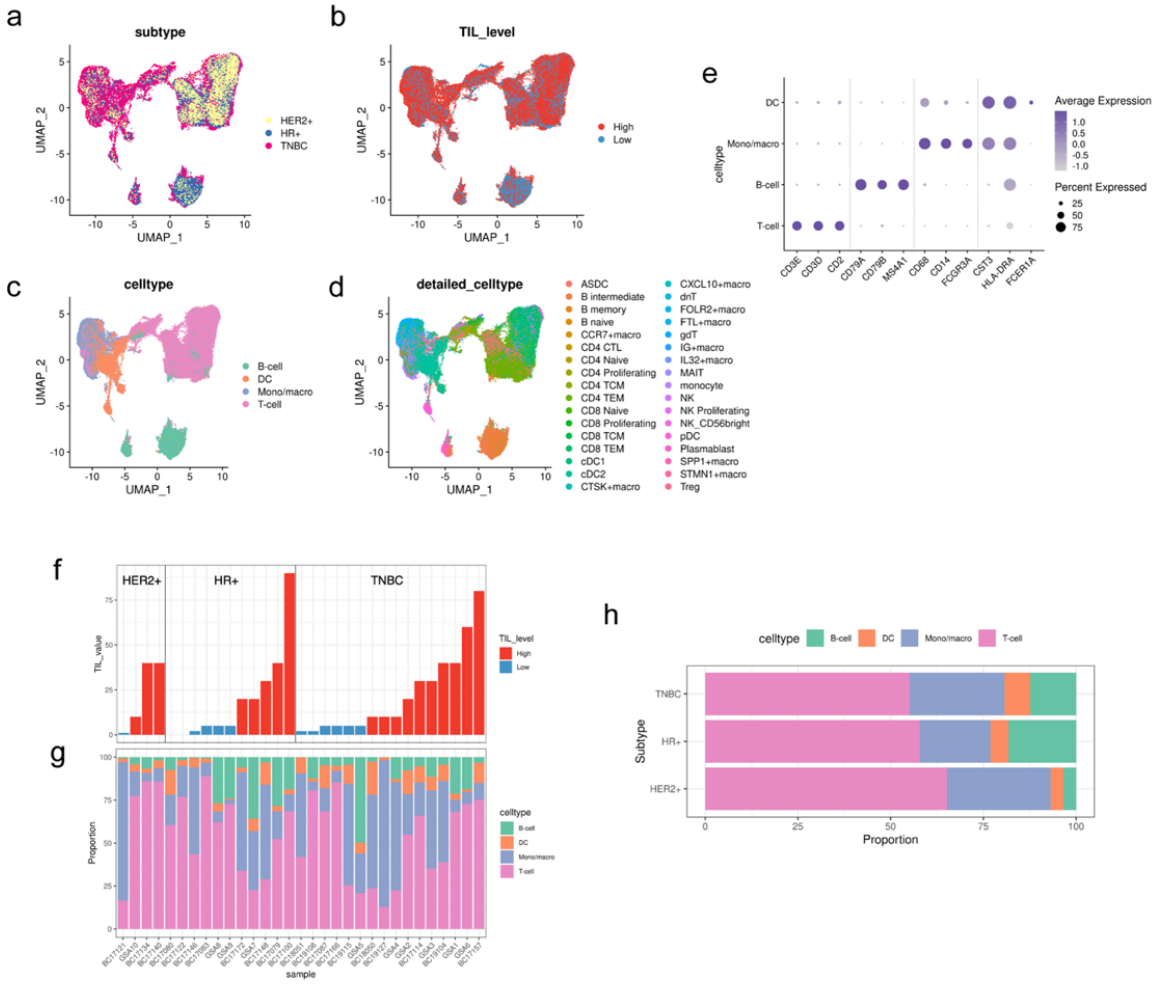

Figure 1. Heterogeneity of immune cell composition in breast cancer.

(a–d) UMAP plot shows breast cancer subtype, TIL levels, cell type, and detailed cell type of 31 samples.

(e) Dot plot shows each major cell type and their expression of selected marker genes.

(f) Bar plot shows TIL value. TIL levels of each sample are represented in colours.

(g) Bar plot shows proportion of cell types in 31 samples.

(h) Bar plot shows proportion of cell types in breast cancer subtypes.

TIL, tumour-infiltrating lymphocytes; DC, dendritic cells; Mono/macro, monocytes, and macrophages.

High proportion of SPP1+ macro in TIL high group of HR+ breast cancer

Our objective was to understand whether and how variations in TIL levels led to differences in immune cell composition. Given that breast cancer shows different characteristics depending on its subtype, we compared the composition within the same breast cancer subtype. Figure 2a–c presents the immune cell distribution of each subtype based on TIL levels. Although each subtype showed different proportions of immune cell subtypes based on TIL levels, these differences were not statistically significant (Figure 2d). Then, we divided cells by major branches (T, B, dendritic cells and mono/macro) and compared the proportions of cells within each branch when further divided into detailed subtypes, based on TIL levels (Figure S2a-c). Mucosal-associated invariant T cells (MAIT) in T-cell ($p = 0.028$) and SPP1+ macro in mono/macro ($p = 0.0043$) in HR+ breast cancer showed statistically significant differences (Figure 2e, f and S2d). MAIT cells was more abundant in the TIL low group while SPP1+ macrophages exhibited higher proportions in the TIL high group. Due to the insufficient number of MAIT cells to perform further comparative analysis, we focused on SPP1+ macrophages. Sub-clustering of HR+ breast cancer mono/macro highlighted the differences in the distribution of SPP1+ macrophage based on the TIL levels (Figure 2g).

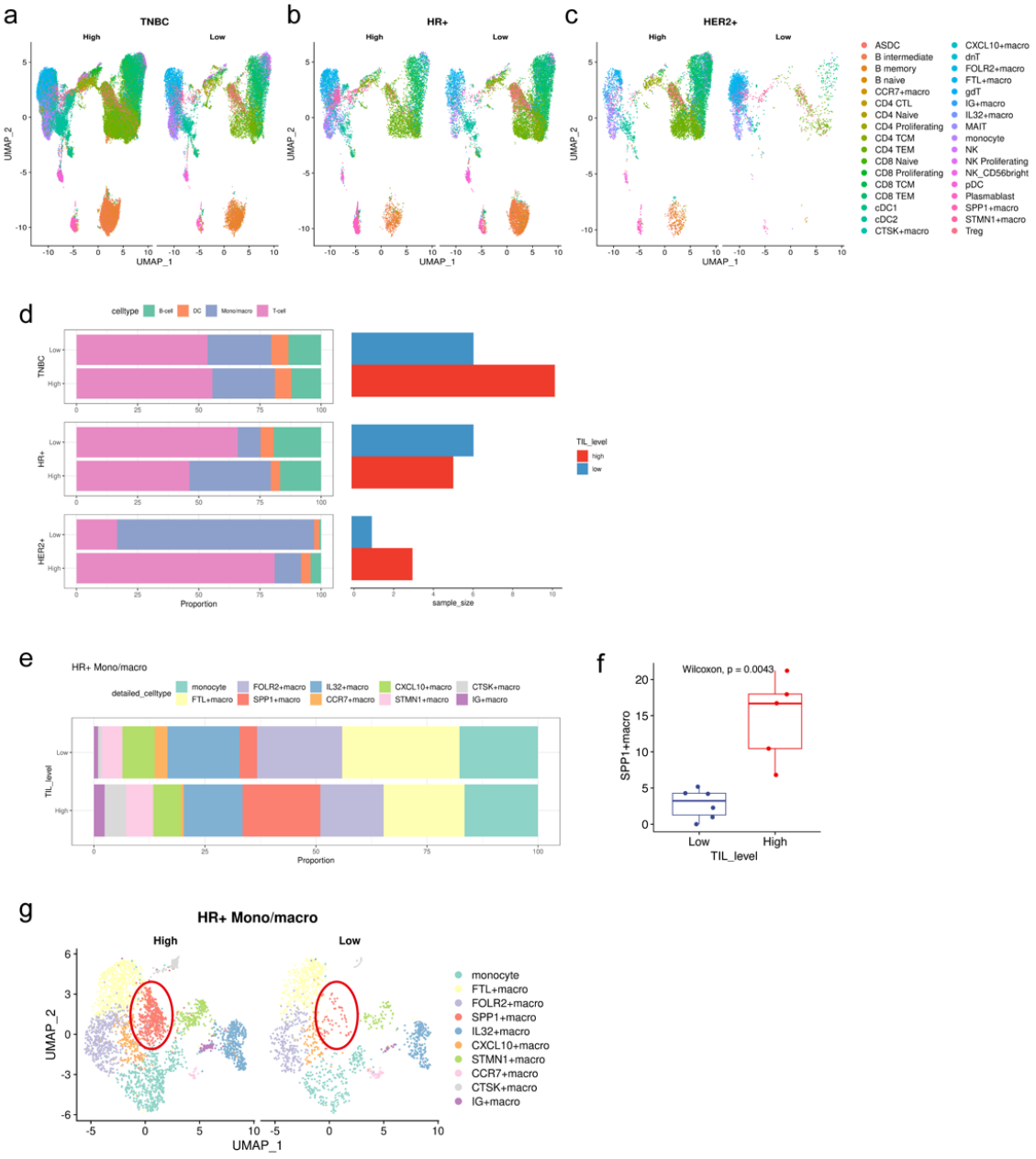

Figure 2. Comparison of cell type proportion by TIL levels revealed increased SPP1+ macrophages in TIL high HR+ breast cancer.

(a–c) UMAP plot shows detailed immune cell subtypes according to TIL levels and breast cancer subtypes.

(d) Bar plot shows cell type proportion of breast cancer subtype in accordance with TIL levels (left), and the corresponding sample size (right).

(e) Bar plot shows proportion of cell types of mono/macro in HR+ breast cancer in accordance with TIL levels.

(f) Boxplot shows proportion of SPP1+macro in accordance with TIL levels (Wilcoxon rank sum test).

(g) UMAP plot shows proportion of mono/macro in HR+ breast cancer in accordance with TIL levels. Red circles indicate the difference in the number of SPP1+ macro.

TIL, tumour-infiltrating lymphocytes; DC, dendritic cells; Mono/macro, monocytes, and macrophages.

TIL high HR+ mono/macro enriched in ECM remodeling-associated pathways with elevated *SPP1* expression

To explore the characteristics of SPP1+ macrophages in HR+ breast cancer, we performed pathway enrichment analysis with DEGs of SPP1+ macrophages with other mono/macro. From the DEG analysis, 24 up-regulated genes including *SPP1*, *CSTB*, *SLC2A1*, and *NURP1* were used for pathway enrichment analysis (Figure 3a). In this analysis, pathways related to ECM remodeling, such as ECM degradation, collagen degradation, and ECM organisation, were significantly enriched in SPP1+ macrophages from HR+ breast cancer (Figure 3b). Similarly, ECM remodeling pathways including ECM degradation, were enriched in SPP1+ macrophages of HR+ breast cancer TIL low group (Figure S3a, b).

To explore whether these characteristics were associated with TIL status, we compared TIL high and low groups within HR+ breast cancer mono/macro subtypes. In 8 out 10 mono/macro cell subtypes, including SPP1+ macrophages, ECM degradation pathway was enriched in the TIL high group (Figure S3c).

To establish whether pathway enrichment related to ECM remodeling was a characteristic of mono/macro from TIL high HR+ breast cancer, we utilised 32 up-regulated genes in the TIL high group for pathway enrichment analysis (Figure 3c). Pathways related to ECM remodeling including ECM degradation and organisation, were enriched in the TIL high group (Figure 3d). A heatmap showing the expression levels of 41 genes involved in ECM degradation revealed that these genes were highly expressed not only in TIL high group SPP1+ macrophages but also in other mono/macro subtypes compared to TIL low group (Figure 3e).

In DEG analysis of HR+ mono/macro, *SPP1* gene was up-regulated in the TIL high group (adjusted *p*-value = 6.128E-273, log2 fold change = 2.963) (Figure 3c). Both feature and violin plots confirmed higher *SPP1* expression in TIL high group compared to TIL low group, and this was not specific to SPP1+ macrophages subtype (Figure 3f). These trends were not observed in other breast cancer subtypes (Figure S3d, e).

In addition, we compared the expression of genes involved in angiogenesis in SPP1+ macrophages and other mono/macrophages to investigate whether SPP1+ macrophages played an angiogenic role, as previously reported [27]. However, we did not observe any significant increase in angiogenic genes within SPP1+ macrophage (Figure S4a–c). Similarly, no positive correlation of *SPP1* expression and angiogenic gene expression was observed in mono/macro (Figure S4d–f). Taken together, TIL high HR+ breast cancer mono/macro exhibited higher expression of *SPP1*, particularly in SPP1+ macrophages subtype, and displayed gene enrichment associated with ECM remodeling.

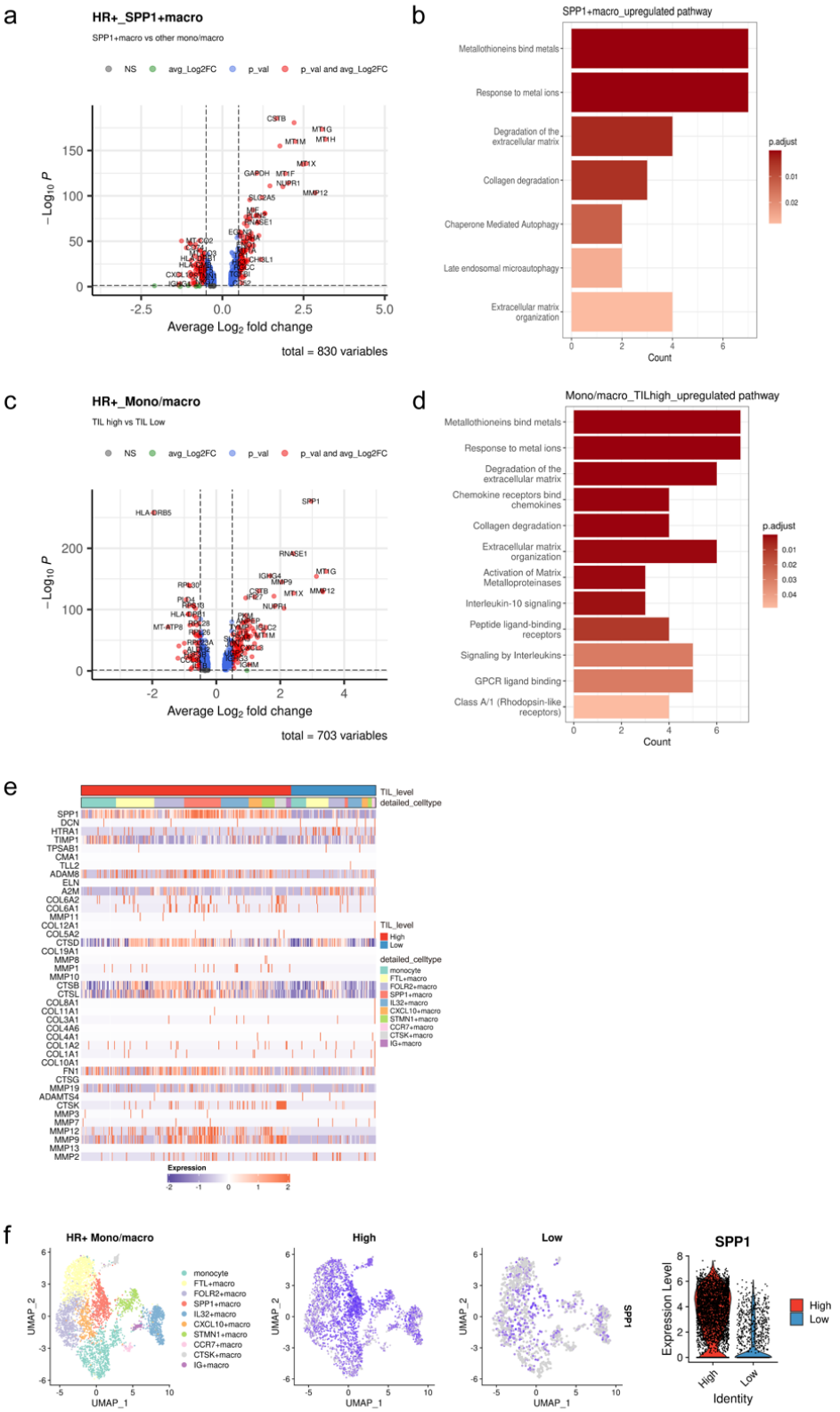

Figure 3. Genes related to ECM remodeling process and *SPP1* are increased in TIL high HR+ breast cancer mono/macro.

(a) Volcano plot of DEGs between SPP1+macro and other mono/macro cell subtypes of HR+ breast cancer. Red dots indicate DEGs.

(b) Bar plot shows enriched pathways of up-regulated genes in SPP1+ macro.

(c) Volcano plot of DEGs between HR+ mono/macro of TIL high and TIL low group. Red dots indicate DEGs.

(d) Bar plot shows enriched pathways of up-regulated genes in TIL high HR+ mono/macro.

(e) UMAP plot shows HR+ mono/macro (left), Feature plot shows level of *SPP1* expression in HR+ Mono/macro in accordance with the TIL levels (middle), Violin plot shows level of *SPP1* expression in HR+ Mono/macro in accordance with the TIL levels (right).

(f) Heatmap of gene expression associated with ECM degradation in HR+ Mono/macro in accordance with the TIL levels and detailed cell type.

DEG, differentially expressed genes; macro, macrophages; mono/macro, monocytes, and macrophages; TIL, tumour-infiltrating lymphocyte; NS, not significant; avg_Log2FC, average $\log_2$ fold change; p_val, p-value; p.adjust, adjusted p-value.

TIL high HR+ Mono/macro interact more with TIL via SPP1 signalling

Cell-to-cell interaction analyses were performed to study the interactions of SPP1+ macrophages with other immune cells using CellChat [24]. We initially compared TIL high and low HR+ breast cancer with differential number of interactions and differential interaction strength (Figure 4a, b). Figure 4a shows that the number of interactions within mono/macro and interactions from mono/macro toward CD8T were more enriched in TIL high group. Moreover, these interactions along with those from mono/macro to CD4T exhibited stronger interaction strengths in the TIL high group (Figure 4b). Comprehensive analysis within the HR+ subtype identified significant enrichment of the SPP1 signalling pathway in the TIL high group (Figure S5a), indicating a potential role of SPP1 gene in immune cell interactions.

To determine which immune cell subtypes interact via *SPP1*, we analysed SPP1 signalling in TIL high and low HR+ breast cancer. In TIL low HR+ breast cancer, SPP1+ macrophages were the primary source (sender) of SPP1, playing a crucial role (Figure 4c). However, in TIL high group, other mono/macro also contributed substantially sources, enabling them to perform a similar function (Figure 4d). Similarly, SPP1+ macrophages had a higher communication probability in SPP1 signalling than other mono/macro subtypes in the TIL low group (Figure 4e), while most of mono/macro displayed similar communication probabilities in the TIL high group (Figure 4f). We proceeded to analyse the role of SPP1 in intercellular communication network and identified the cell types involved in this process. In TIL low group, SPP1+ macrophages were the major sender (Figure 4g), but in TIL high group, various mono/macro subtypes acted as senders of SPP1 signalling (Figure 4h). Additionally, T cells tended to act as the major receiver in SPP1 signalling in TIL high group (Figure 4h).

To determine which ligand-receptor pairs are important in SPP1 signalling, we analysed the contribution of each pair in the SPP1 signalling pathway (Figure S5b, c). *SPP1-CD44* was the highest contribution in both TIL high and low groups. The receptor action of *ITGA+ITGB* to *SPP1* was more pronounced in the TIL high group compared to the low group. While *SPP1* expression level was higher in the TIL high group, *CD44* levels remained similar between the TIL high and low groups. Furthermore, the expression level of *ITGB1* was elevated in TIL high group (Figure S5d, e).

Additionally, we examined the expression of immunosuppression and proliferation-related markers in T cells based on the expression of *SPP1* in mono/macro to evaluate the impact of SPP1 signalling on T cells. The analysis revealed no significant differences (Figure S6a–c). Collectively, these findings underscored the significant role of *SPP1* in intercellular interaction between mono/macro and T cells in TIL high HR+ breast cancer.

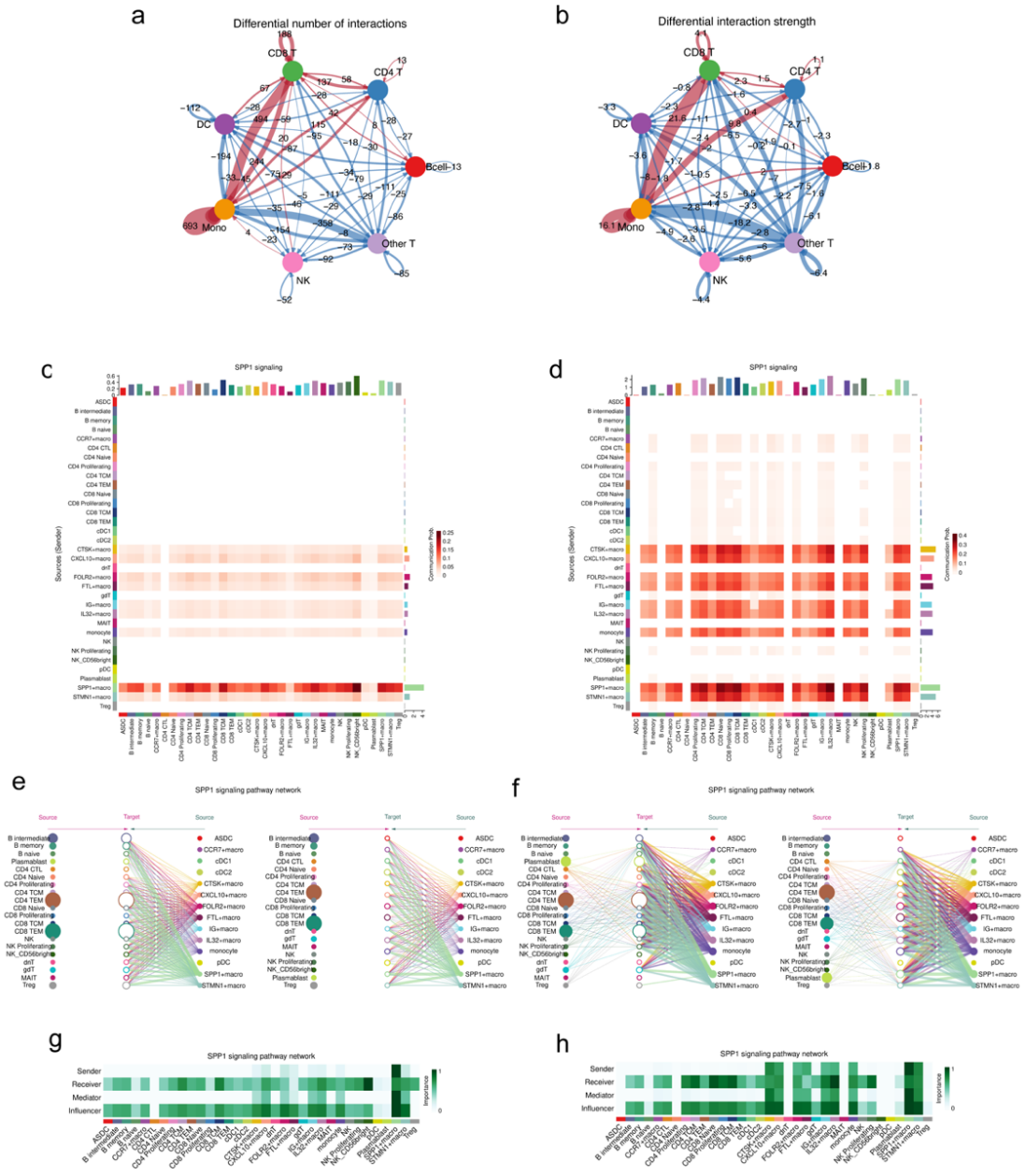

Figure 4. Cell-to-cell interaction comparison analysis between TIL high HR+ breast cancer and TIL low group.

(a) Differential number of interactions between TIL high and TIL low. Arrow represents direction, coloured edges indicate increased signalling in TIL high (red) or TIL low (blue) and line width reflects strength value.

(b) Differential interaction strength between TIL high and TIL low, Arrow represents direction, coloured edges indicate increased signalling in TIL high (red) or TIL low (blue) and line width reflects interaction number.

(c) Communication probability of SPP1 signalling network of source (sender) (rows) across target (columns) in TIL low.

(d) Communication probability of SPP1 signalling network in TIL high.

(e) Hierarchy plot shows cell-cell communication network of SPP1 signalling in TIL low. Circle size indicates each cell group proportion and edge width represents communication probability.

(f) Cell-cell communication network of SPP1 signalling in TIL high.

(g) Heatmaps show relative importance of each cell group across signalling roles in TIL low and (h) relative importance of each cell group across signalling roles in TIL high.

TIL, tumour-infiltrating lymphocyte; mono/macro, monocytes, and macrophages; CD4T, CD4+ T cells; CD8T, CD8+ T cells; NK, NK T cells; OtherT, other T cells.

Spatial colocalization of mono/macro and CD8T/CD4T in TIL high HR+ breast cancer

Through cell-to-cell interaction analysis, we demonstrated differential interactions between mono/macro and CD8T/CD4T in TIL high and low HR+ breast cancer. Furthermore, we identified mono/macro as sender, and CD8T/CD4T as receivers in SPP1 signalling. To explore the spatial proximity of these cells for potential interactions, we utilised two spatial transcriptomics datasets of HR+ breast cancer [25]. They were classified as TIL high (CID4535) and TIL low (CID4290) based on H&E images (Figure 5a, c). We confirmed appropriate pathologic annotations were done to determine the distribution of invasive cancer, stroma, lymphocyte, and other components in deconvoluted classification. (Figure 5b, d).

Subsequently, we employed signature scoring of cell subtypes using the top 25 genes to annotate the spots obtained through spatial transcriptomics. These scores were then utilised for conducting correlation analyses across the scores in each spot. Signature scores of mono/macro, CD8T, and CD4T were calculated using our scRNA-seq data of CD45+ breast cancer (Figure 5e, f). To validate the legitimacy of the signature score of our CD45+ sorted dataset, we employed a public non-sorted scRNA-seq dataset (GSE176078) to establish additional signature score criterion [28]. Comparing the distribution of signature scores calculated from the public dataset with our dataset, we found no significant differences (Figure S7c–f). Then, we analysed the correlation of signature scores in each spot of interest. The correlation between mono/macro score and CD8T score (R^2=0.52), and mono/macro score and CD4T score (R^2=0.43) was higher in the TIL high group than that in the low group (R^2 = 0.045 and 0.017, respectively) (Figure 5g, h). These results showed that in TIL high group, macro/mono and CD8T/CD4T were more likely in the same spot compared to TIL low group, implying their colocalization.

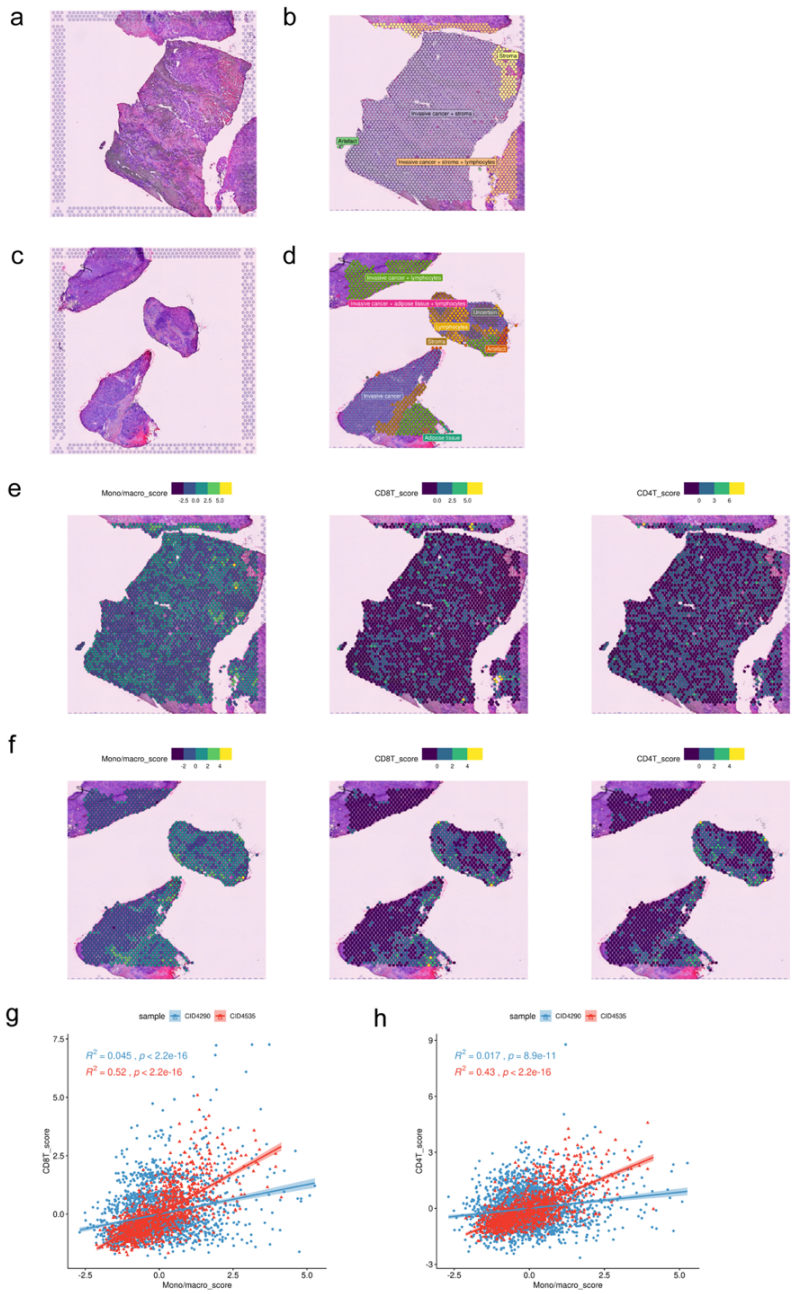

Figure 5. Mono/macro and CD8T/CD4T are spatially colocalised in TIL high HR+ breast cancer.

(a, c) H&E image of tissue section analysed using VISIUM.

(b, d) Classification of VISIUM public dataset.

(e, f) Signature score of Mono/macro, CD8T, and CD4T.

(g, h) Correlation of signature scores (Spearman's correlation coefficient).

Mono/macro, monocytes, and macrophages; CD8T, CD8+ T cells; CD4T, CD4+ T cells; TIL, tumour-infiltrating lymphocyte.

Discussion

Here, we highlighted the abundance of *SPP1*-expressing macrophages in TIL high HR+ breast cancer, and their heightened interaction with colocalised T cells through SPP1 signalling.

The *SPP1* gene encodes osteopontin, a matricellular protein previously associated with promoting angiogenesis in breast cancer [29]. Single cell studies have indicated that SPP1+ macrophages interact with FAP+ fibroblasts in colon cancer, exhibiting a pro-angiogenic signature [27, 30]. However, our study revealed that SPP1+ macrophages did not exhibit higher expression of angiogenic marker genes, and *SPP1* expression in macrophages was not correlated with the expression of angiogenic marker genes. This pattern remained consistent across all breast cancer subtypes. Thus, in breast cancer, SPP1+ macrophages may serve roles other than angiogenesis.

In this research, we proposed a novel role of *SPP1* within tumour-associated macrophages in breast cancer, shedding light on their primary interaction mediated by SPP1 signalling with other immune cells. This signalling pathway was associated with cancer-promoting pathways in gastric cancer [31], and was linked to TAM infiltrations and poor prognosis in glioma [32]. However, these studies mainly focused on the role of SPP1+ macrophages in their interaction with tumour epithelial cells. In a recent study involving ovarian cancer, *SPP1* expression was associated with higher TIL levels, but also with increased immune checkpoint marker gene expression and poor prognosis, potentially indicating immune tolerance [33]. Unfortunately, this study did not specify the cell types responsible for these expression changes. We could not identify any significant correlation between heightened *SPP1* expression in macrophages and immune checkpoint marker gene expression or cell cycle progression scores in T cells. Additionally, Tregs did not appear as the primary recipients of SPP1 signalling in TIL high HR+ breast cancer. Therefore, it is plausible that the impact of macrophage-derived *SPP1* on T cells may not be associated with immune suppression, and further research is needed to ascertain their precise role.

SPP1+ macrophages have previously been associated with fibrogenesis in chronic inflammation [34, 35] and a higher metastatic rate in cancer [36, 37]. To examine how macrophage function affects TILs, we conducted DEG analyses. Both SPP1+ macrophages and monocytes/macrophages in TIL high HR+ breast cancer showed upregulation of genes related to ECM

degradation compared to other monocytes/macrophages and those in the TIL low group. These findings suggest an increased ECM remodeling process in TIL high HR+ breast cancer, potentially facilitating tumour invasion and metastasis [38]. Although the precise mechanism underlying this up-regulated ECM remodeling in macrophages in TIL high HR+ breast cancer remains unclear, it could potentially contribute to the unfavourable prognosis associated with this subtype.

In contrast to other breast cancer subtypes, patients with HR+ breast cancer having higher TIL levels are associated with worse prognosis [7, 8]. However, after receiving chemotherapy, patients having higher TIL levels are associated with higher pCR rates along with longer disease-free survival [7, 39]. While our study suggests increased *SPP1* expression in macrophages as a unique characteristic of TIL high HR+ breast cancer that may impact TILs, ECM remodeling and prognosis, all patients with HR+ breast cancer included in our study were untreated, which limits our ability to assess the impact of chemotherapy on the TME and its association with prognosis. Notably, recent research has indicated an elevated risk of recurrence in tamoxifen-treated HR+ breast cancer cases with high *SPP1* mRNA expression in bulk tumour tissue [40]. This association may be attributed to the previously mentioned immunosuppressive and ECM remodeling effects of SPP1+ macrophages [33, 38]. Therefore, a potential strategy to enhance the prognosis of patients with TIL high HR+ breast cancer could involve combining drugs that target *SPP1* with the current chemotherapy regimen.

Currently, there are no commercially available drugs for *SPP1* inhibition. However, based on our investigation utilising the Drug Gene Budger (DGB) [41], daunorubicin was identified as a potential agent capable of reducing *SPP1* expression in acute myeloid leukaemia cell lines such as SKM1. Nonetheless, further research is imperative for drug development, as daunorubicin did not exhibit similar effects in other cell lines within the DGB database.

In conclusion, we demonstrated that increased *SPP1* expression in monocytes/macrophages in TIL high HR+ breast cancer may directly influence TILs, potentially enhancing ECM remodeling and T cell interactions. Therefore, targeting SPP1+ macrophages could offer a promising approach to ameliorate the poor prognosis associated with TIL high HR+ breast cancer.

Acknowledgements

This study was supported by the Asan Institute for Life Sciences, Asan Medical Center, Seoul, Korea (2019-732 and 2020-732) and Basic Science Research Programs through the National Research Foundation of Korea (NRF), funded by the Ministry of Science, ICT & Future Planning, Korea (NRF-2018R1D1A1B07048831).

References

1. Ferlay J, Ervik M, Lam F, et al. Global Cancer Observatory: Cancer Today Lyon, France: International Agency for Research on Cancer2020 [Available from: https://gco.iarc.fr/today.
2. Loibl S, Poortmans P, Morrow M, et al. Breast cancer. Lancet. 2021;397(10286):1750-69.
3. Loi S, Michiels S, Adams S, et al. The journey of tumor-infiltrating lymphocytes as a biomarker in breast cancer: clinical utility in an era of checkpoint inhibition. Ann Oncol. 2021;32(10):1236-44.
4. Salgado R, Denkert C, Demaria S, et al. The evaluation of tumor-infiltrating lymphocytes (TILs) in breast cancer: recommendations by an International TILs Working Group 2014. Ann Oncol. 2015;26(2):259-71.
5. Stanton SE, Adams S, Disis ML. Variation in the Incidence and Magnitude of Tumor-Infiltrating Lymphocytes in Breast Cancer Subtypes: A Systematic Review. JAMA Oncol. 2016;2(10):1354-60.
6. Gao ZH, Li CX, Liu M, et al. Predictive and prognostic role of tumour-infiltrating lymphocytes in breast cancer patients with different molecular subtypes: a meta-analysis. BMC Cancer. 2020;20(1):1150.
7. Denkert C, von Minckwitz G, Darb-Esfahani S, et al. Tumour-infiltrating lymphocytes and prognosis in different subtypes of breast cancer: a pooled analysis of 3771 patients treated with neoadjuvant therapy. Lancet Oncol. 2018;19(1):40-50.
8. Makhlouf S, Wahab N, Toss M, et al. Evaluation of tumour infiltrating lymphocytes in luminal breast cancer using artificial intelligence. Br J Cancer. 2023.
9. Labani-Motlagh A, Ashja-Mahdavi M, Loskog A. The Tumor Microenvironment: A Milieu Hindering and Obstructing Antitumor Immune Responses. Front Immunol. 2020;11:940.
10. Qiu SQ, Waaijer SJH, Zwager MC, et al. Tumor-associated macrophages in breast cancer: Innocent bystander or important player? Cancer Treat Rev. 2018;70:178-89.
11. Christofides A, Strauss L, Yeo A, et al. The complex role of tumor-infiltrating macrophages. Nat Immunol. 2022;23(8):1148-56.
12. Timperi E, Gueguen P, Molgora M, et al. Lipid-Associated Macrophages Are Induced by Cancer-Associated Fibroblasts and Mediate Immune Suppression in Breast Cancer. Cancer Res. 2022;82(18):3291-306.
13. Nalio Ramos R, Missolo-Koussou Y, Gerber-Ferder Y, et al. Tissue-resident FOLR2(+) macrophages associate with CD8(+) T cell infiltration in human breast cancer. Cell. 2022;185(7):1189-207 e25.
14. Goldberg J, Pastorello RG, Vallius T, et al. The Immunology of Hormone Receptor Positive Breast Cancer. Front Immunol. 2021;12:674192.
15. Bense RD, Sotiriou C, Piccart-Gebhart MJ, et al. Relevance of Tumor-Infiltrating Immune Cell Composition and Functionality for Disease Outcome in Breast Cancer. J Natl Cancer Inst. 2017;109(1).
16. Hu Q, Hong Y, Qi P, et al. Atlas of breast cancer infiltrated B-lymphocytes revealed by paired single-cell RNA-sequencing and antigen receptor profiling. Nat Commun. 2021;12(1):2186.
17. Zheng GX, Terry JM, Belgrader P, et al. Massively parallel digital transcriptional profiling of single cells. Nat Commun. 2017;8(1):14049.
18. Hao Y, Hao S, Andersen-Nissen E, et al. Integrated analysis of multimodal single-cell data. Cell. 2021;184(13):3573-87 e29.
19. Team RC. R: A Language and Environment for Statistical Computing: R Foundation for Statistical Computing; 2021 [Available from: https://www.R-project.org/.
20. Korsunsky I, Millard N, Fan J, et al. Fast, sensitive and accurate integration of single-cell data with Harmony. Nat Methods. 2019;16(12):1289-96.

21. Andrew B, Charlotte D, Yuhan H, et al. Azimuth: A Shiny App Demonstrating a Query-Reference Mapping Algorithm for Single-Cell Data 2022 [Available from: https://github.com/satijalab/azimuth.
22. Yu G, He QY. ReactomePA: an R/Bioconductor package for reactome pathway analysis and visualization. Mol Biosyst. 2016;12(2):477-9.
23. Wickham H. ggplot2: Elegant Graphics for Data Analysis: Springer-Verlag New York; 2016 [Available from: https://ggplot2.tidyverse.org.
24. Jin S, Guerrero-Juarez CF, Zhang L, et al. Inference and analysis of cell-cell communication using CellChat. Nat Commun. 2021;12(1):1088.
25. Sunny ZW, Alexander S. A single-cell and spatially resolved atlas of human breast cancers | spatial transcriptomics data. Nature Genetics2021.
26. Kassambara A. ggpubr: 'ggplot2' Based Publication Ready Plots. 2023.
27. Ma RY, Black A, Qian BZ. Macrophage diversity in cancer revisited in the era of single-cell omics. Trends Immunol. 2022;43(7):546-63.
28. Wu SZ, Al-Eryani G, Roden DL, et al. A single-cell and spatially resolved atlas of human breast cancers. Nat Genet. 2021;53(9):1334-47.
29. Chakraborty G, Jain S, Kundu GC. Osteopontin promotes vascular endothelial growth factor-dependent breast tumor growth and angiogenesis via autocrine and paracrine mechanisms. Cancer Res. 2008;68(1):152-61.
30. Qi J, Sun H, Zhang Y, et al. Single-cell and spatial analysis reveal interaction of FAP(+) fibroblasts and SPP1(+) macrophages in colorectal cancer. Nat Commun. 2022;13(1):1742.
31. Xie W, Cheng J, Hong Z, et al. Multi-Transcriptomic Analysis Reveals the Heterogeneity and Tumor-Promoting Role of SPP1/CD44-Mediated Intratumoral Crosstalk in Gastric Cancer. Cancers (Basel). 2022;15(1).
32. He C, Sheng L, Pan D, et al. Single-Cell Transcriptomic Analysis Revealed a Critical Role of SPP1/CD44-Mediated Crosstalk Between Macrophages and Cancer Cells in Glioma. Front Cell Dev Biol. 2021;9:779319.
33. Gao W, Liu D, Sun H, et al. SPP1 is a prognostic related biomarker and correlated with tumor-infiltrating immune cells in ovarian cancer. BMC Cancer. 2022;22(1):1367.
34. Hoeft K, Schaefer GJL, Kim H, et al. Platelet-instructed SPP1(+) macrophages drive myofibroblast activation in fibrosis in a CXCL4-dependent manner. Cell Rep. 2023;42(2):112131.
35. Morse C, Tabib T, Sembrat J, et al. Proliferating SPP1/MERTK-expressing macrophages in idiopathic pulmonary fibrosis. Eur Respir J. 2019;54(2).
36. Sangaletti S, Tripodo C, Sandri S, et al. Osteopontin shapes immunosuppression in the metastatic niche. Cancer Res. 2014;74(17):4706-19.
37. Zhang C, Wu M, Zhang L, et al. Fibrotic microenvironment promotes the metastatic seeding of tumor cells via activating the fibronectin 1/secreted phosphoprotein 1-integrin signaling. Oncotarget. 2016;7(29):45702-14.
38. Yuan Z, Li Y, Zhang S, et al. Extracellular matrix remodeling in tumor progression and immune escape: from mechanisms to treatments. Mol Cancer. 2023;22(1):48.
39. Criscitiello C, Vingiani A, Maisonneuve P, et al. Tumor-infiltrating lymphocytes (TILs) in ER+/HER2- breast cancer. Breast Cancer Res Treat. 2020;183(2):347-54.
40. Gothlin Eremo A, Lagergren K, Othman L, et al. Evaluation of SPP1/osteopontin expression as predictor of recurrence in tamoxifen treated breast cancer. Sci Rep. 2020;10(1):1451.
41. Wang Z, He E, Sani K, et al. Drug Gene Budger (DGB): an application for ranking drugs to modulate a specific gene based on transcriptomic signatures. Bioinformatics. 2019;35(7):1247-8.

Supplementary information

Table S1. Clinical information of breast cancer patients involved in the study.

subtype	TIL level	Sample Name	TIL value	cell counts
TNBC	High	BC17157	80	2440
		GSA6	60	15739
		BC19104	40	3384
		GSA1	40	9249
		BC17114	30	2059
		GSA3	30	4624
		GSA2	20	10637
		BC18050	10	2695
		BC19127	10	4133
		GSA4	10	1074
	Low	BC17087	5	2172
		BC17166	5	3512
		BC19115	5	3462
		GSA5	5	3077
		BC18051	2	2317
		BC19108	2	2984
HR+	High	BC17100	90	2380
		BC17079	40	2960
		BC17148	30	767
		BC17172	20	3638
		GSA7	20	524
	Low	BC17083	5	218
		GSA8	5	4953
		GSA9	5	5268
		BC17146	2	459
		BC17080	0	3271
		BC17122	0	593
HER2+	High	BC17134	40	2035
		BC17140	40	1703
		GSA10	10	4919
	Low	BC17121	1	2813

TNBC, Triple-negative breast cancer; HR+, Hormone receptor-positive breast cancer; HER2+, HER2-positive breast cancer.

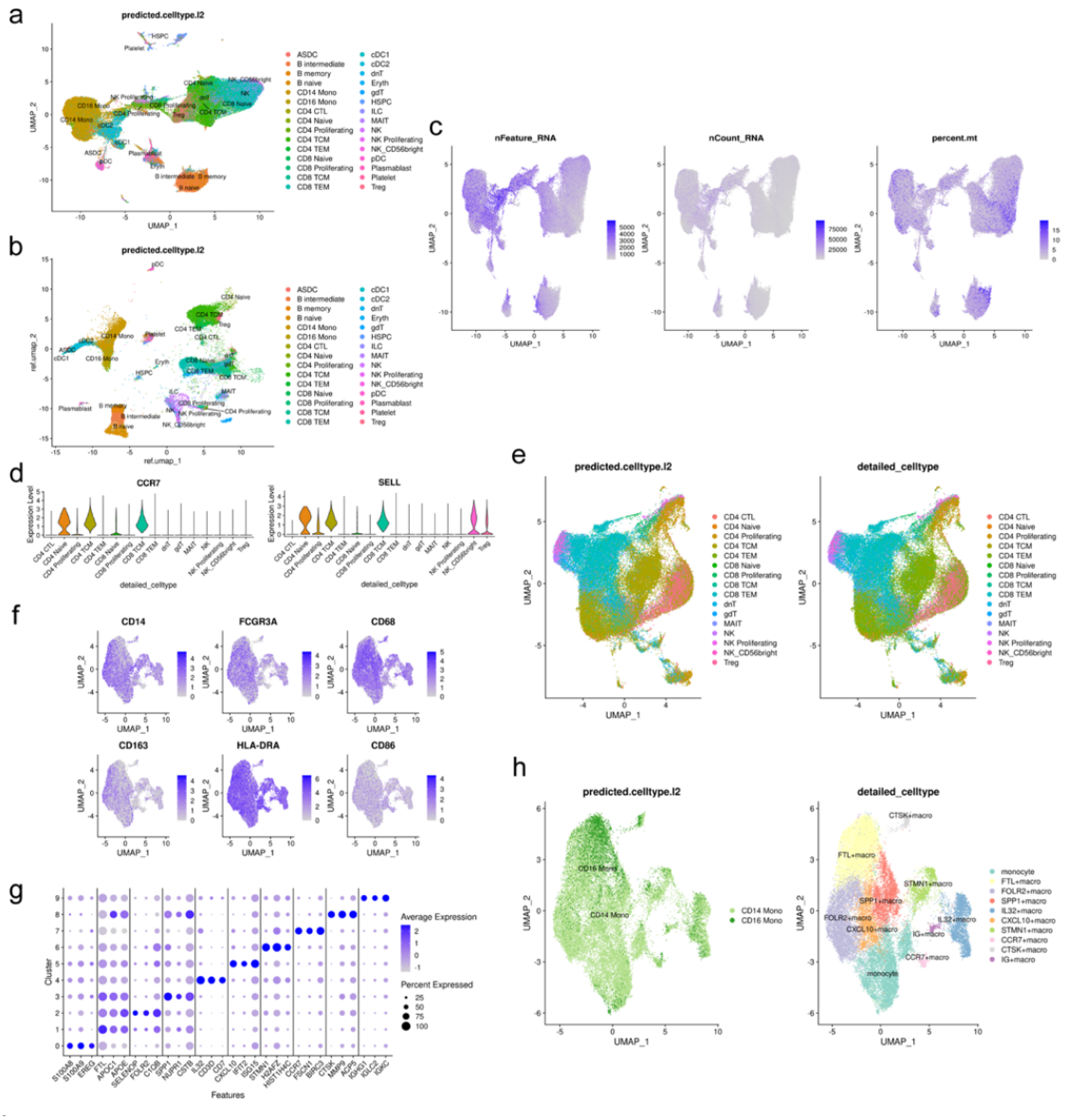

Figure S1. Sample quality control and detailed annotation of immune cells.

(a) UMAP plot shows predicted cell type l2 by Azimuth.

(b) UMAP plot shows predicted cell type l2 represented by ref.umap.

(c) Feature plot shows percent.mt, nFeature_RNA and ncount_RNA.

(d) Expression level of *CCR7* and *SELL* in T-cell

(e) UMAP plot shows predicted cell type l2 by Azimuth (left) and detailed cell type (right) in T-cell.

(f) Expression level of canonical markers of monocyte and macrophages in mono/macro.

(g) Dot plot shows expression level of gene signature of clusters in mono/macro.

(h) UMAP plot shows predicted cell type l2 by Azimuth (left) and detailed cell type (right) in Mono/macro.

Mono/macro, monocytes, and macrophages; DC, dendritic cells.

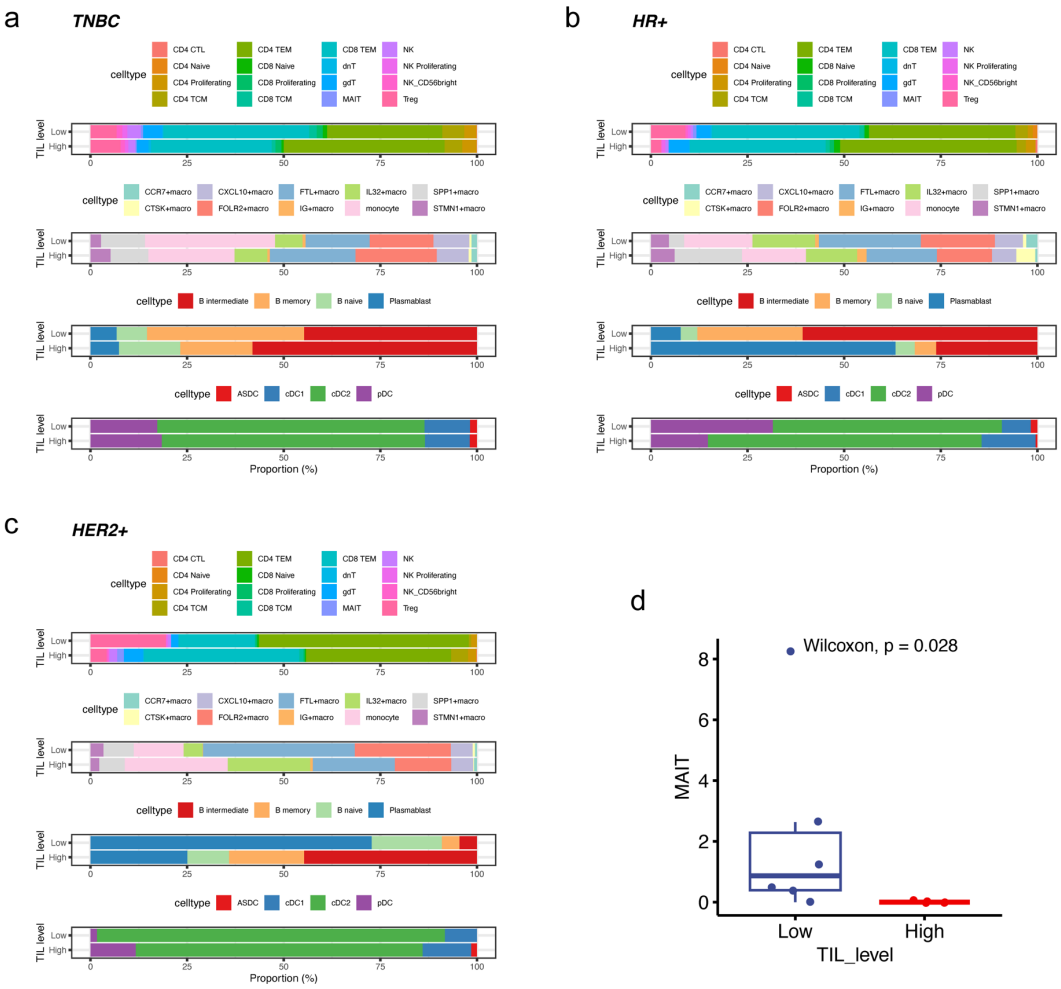

Figure S2. Proportion of immune cells in different subtypes of breast cancer.

(a–c) Bar plot shows proportion of each cell type across TIL levels.

(d) Boxplot shows proportion of MAIT in HR+ subtype across TIL levels (Wilcoxon rank sum test)

TIL, tumour-infiltrating lymphocytes; MAIT, mucosal-associated invariant T cells.

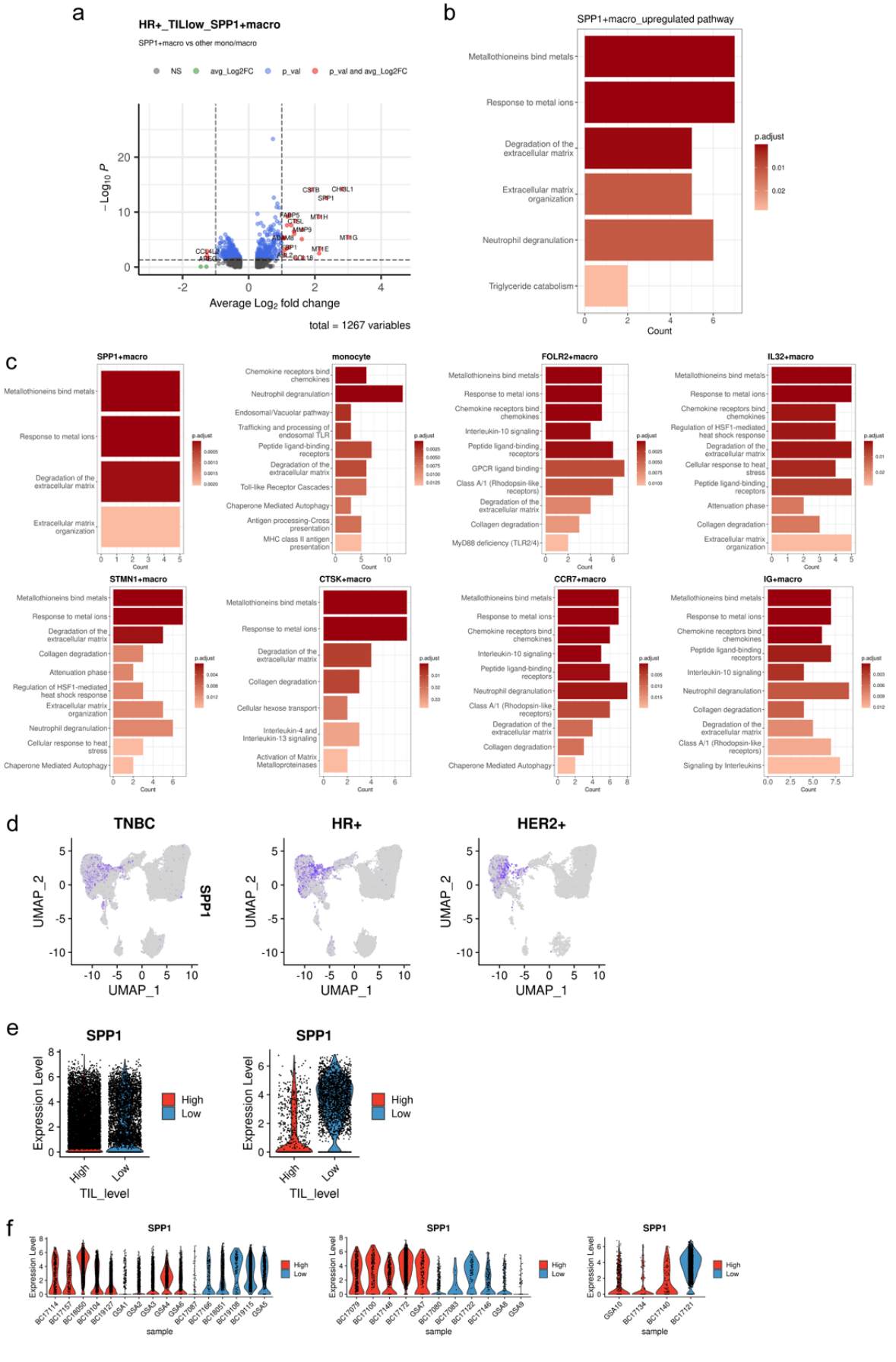

Figure S3. Supplementary data for pathway enrichment analysis and *SPP1* expression in breast cancer.

(a) Volcano plot of DEGs between SPP1+ macro and other mono/macro cell types of TIL low group in HR+ subtype. Red dots indicate DEGs.

(b) Bar plot shows enriched pathways of up-regulated genes of DEG analysis between SPP1+ macro and other mono/macro cell types of TIL low group in HR+ subtype.

(c) Bar plots show enriched pathways of up-regulated genes of DEG analysis between TIL high and TIL low of each mono/macro subtype in HR+ breast cancer.

(d) Feature plot shows *SPP1* expression level in each breast cancer subtype.

(e) Expression level of *SPP1* in TNBC and HER2+ subtype across TIL levels.

(f) Expression level of *SPP1* in TNBC, HR+ and HER2+ subtype across samples.

DEG, differentially expressed gene; macro, macrophages; mono/macro, monocytes, and macrophages; TIL, tumour-infiltrating lymphocytes; NS, not significant; avg_Log2FC, average $\log_2$ fold change; p_val, p-value; p.adjust, adjusted p-value.

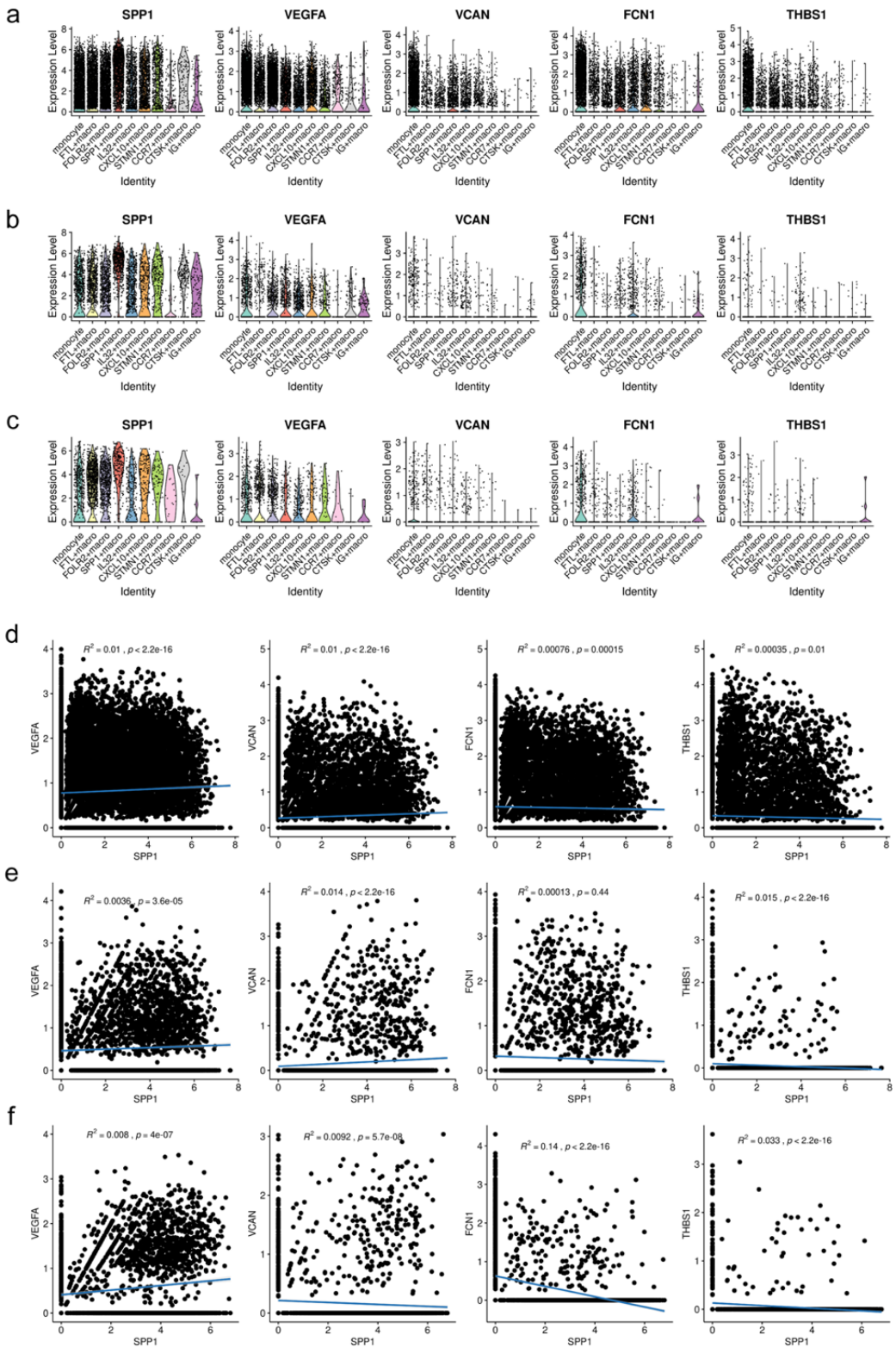

Figure S4. ***SPP1*** **expression of mono/macro was not associated with the expression of angiogenic markers in breast cancer.**

(a) Violin plot showing expression level of genes in mono/macro of TNBC.

(b) Violin plot showing expression level of genes in mono/macro of HR+ subtype.

(c) Violin plot showing expression level of genes in mono/macro of HER2+ subtype.

(d) Correlation of SPP1 and angiogenic markers (*VEGFA*, *VCAN*, *FCN1*, and *THBS1*) in mono/macro of TNBC (Spearman correlation coefficient).

(e) Correlation of SPP1 and angiogenic markers (*VEGFA*, *VCAN*, *FCN1*, and *THBS1*) in mono/macro of HR+ subtype (Spearman correlation coefficient).

(f) Correlation of SPP1 and angiogenic markers (*VEGFA*, *VCAN*, *FCN1*, and *THBS1*) in mono/macro of HER2+ subtype (Spearman correlation coefficient).

Mono/macro, monocytes, and macrophages.

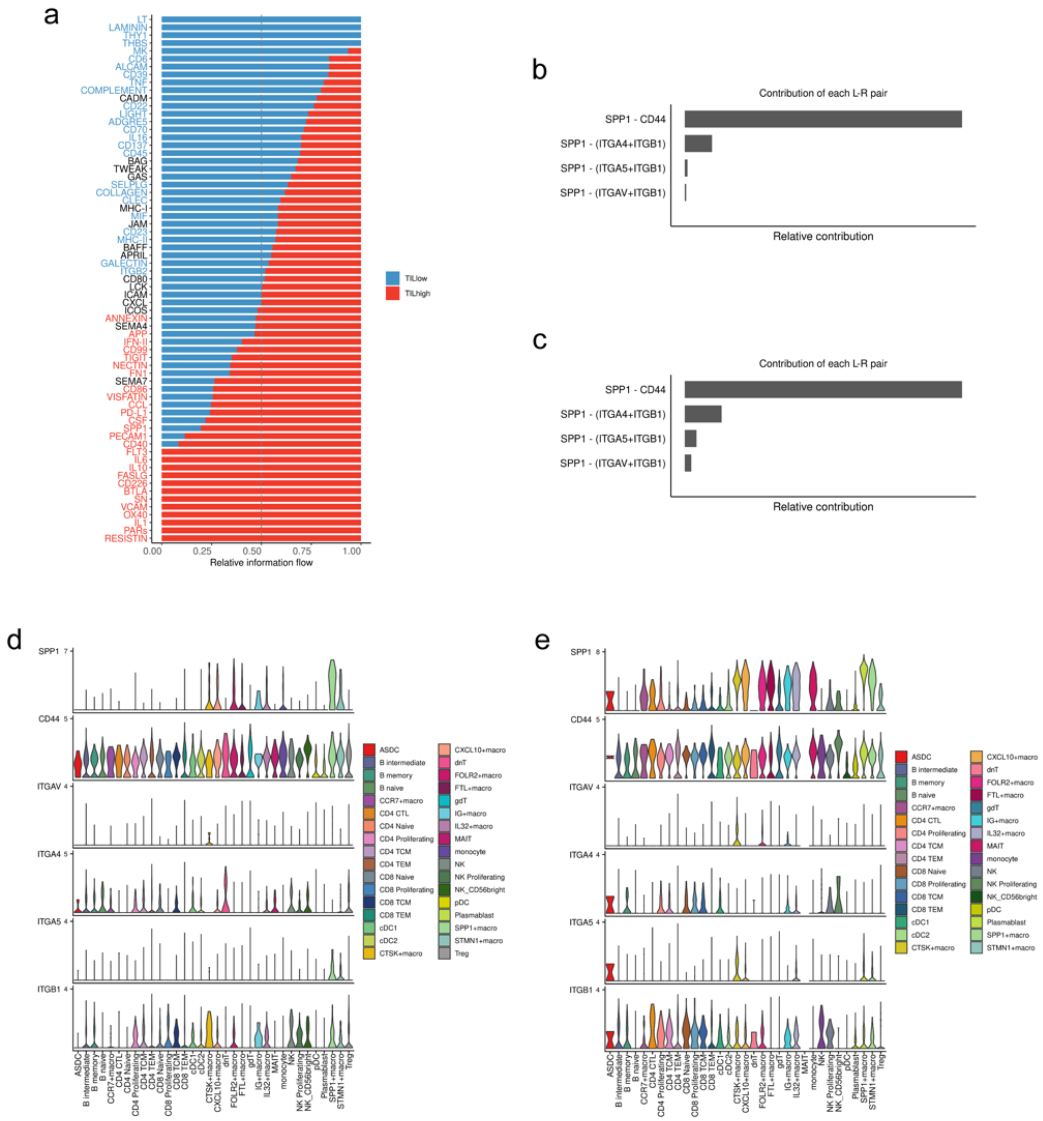

Figure S5. Supplementary data for cell-to-cell interaction analysis.

(a) Bar plot shows all significant signalling pathways that are ranked based on their differences of overall information flow between TIL high and TIL low groups in HR+ breast cancer. The signalling pathways coloured by red are more enriched in TIL high group, the black ones are equally enriched in TIL high and TIL low groups, and the blue ones are more enriched in TIL low group.

(b) Relative contribution of each ligand-receptor pair to the SPP1 signalling network in TIL low HR+ breast cancer.

(c) Relative contribution of each ligand-receptor pair to the SPP1 signalling network in TIL high HR+ breast cancer.

(d) Violin plot shows expression levels of ligand and receptors of the SPP1 signalling in TIL low HR+ breast cancer.

(e) Violin plot shows expression levels of ligand and receptors of the SPP1 signalling in TIL high HR+ breast cancer.

TIL, tumour-infiltrating lymphocytes.

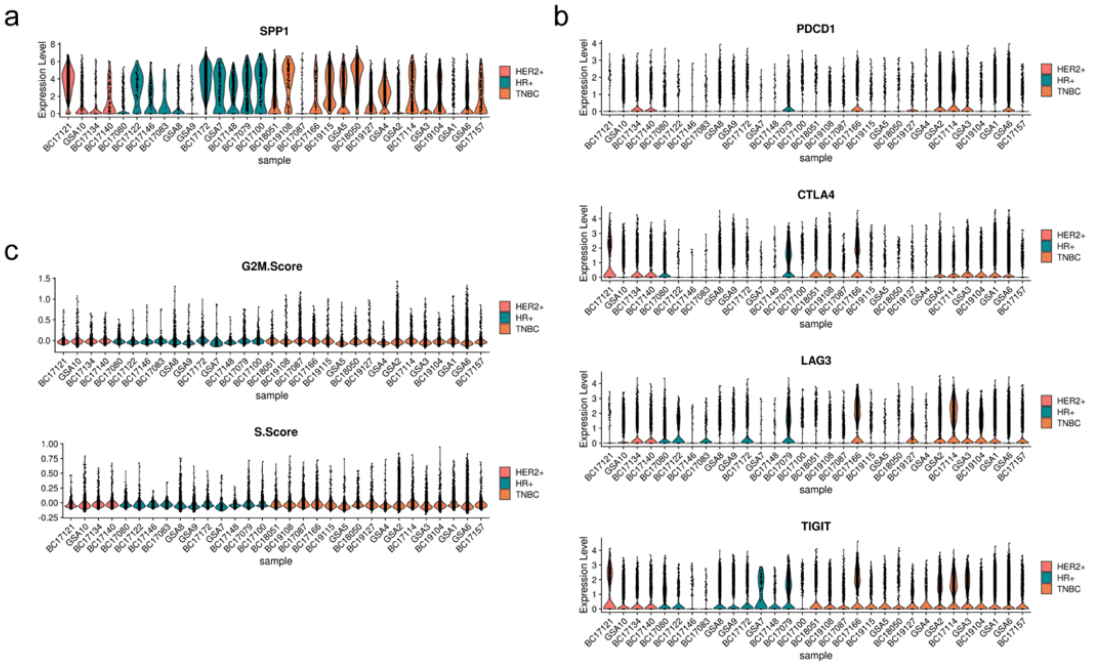

Figure S6. *SPP1* expression of mono/macro was associated with neither cell cycle score nor expression of immune checkpoint markers of T cells in breast cancer.

(a) Expression level of *SPP1* of each sample in mono/macro.

(b) Expression level of immune checkpoint molecules (*PDCD1*, *LAG3*, *CTLA4* and *TIGIT*) of each sample in T cells.

(c) Violin plot showing cell cycle score of each sample in T cells.

Mono/macro, monocytes, and macrophages.

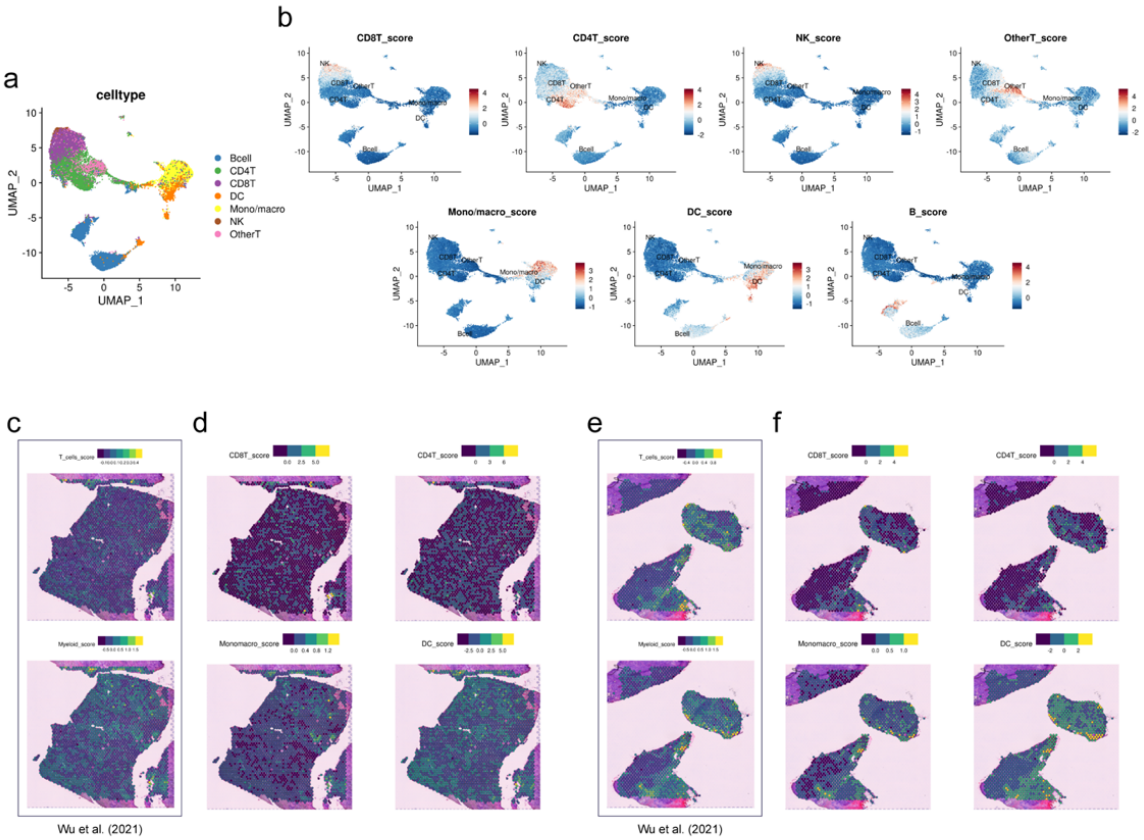

Figure S7. Signature scoring in VISIUM.

(a) UMAP plot shows cell types of HR+ subtype. T cells were divided into four groups.

(b) Feature plots show signature score of each cell type in HR+ subtype.

(c) Signature score represented in CID4290. Signature genes are derived from GSE176078 (ER+ subtype).

(d) Signature score represented in CID4290. Signature genes are derived from our HR+ subtype data.

(e) Signature score represented in CID4535. Signature genes are derived from GSE176078 (ER+ subtype).

(f) Signature score represented in CID4535. Signature genes are derived from our HR+ subtype data.

국문요약

유방암은 세계적으로 가장 흔한 암이며, 호르몬 수용체와 HER2 수용체의 발현에 따라 호르몬 수용체 양성(HR+), 사람 상피세포 성장인자 수용체 양성(HER2+), 삼중음성 유방암의 세 가지 아형으로 나뉠 수 있다. 유방암에서 종양침윤림프구 (TIL)의 수준은 중요한 예후 인자이다. 유방암의 아형에 따른 TIL 수준의 다양한 역할을 분석하고 종양미세환경과 면역세포 구성이 미치는 영향을 조사하기 위해, 31명의 환자의 유방암 조직에서 단일세포전사체 분석을 시행하였다. 그 결과 높은 TIL 수준을 가진 HR+ 유방암에서 SPP1+ 대식세포가 증가하였고 점막연관 불변사슬 T세포 (MAIT)가 감소한 것을 관찰하였다. 또한, SPP1 발현은 높은 TIL 수준의 HR+ 유방암의 다른 단핵구 및 대식세포 하위 그룹에서도 증가 하였으며, SPP1+ 대식세포와 높은 TIL 수준의 HR+ 유방암의 단핵구 및 대식세포 모두에서 세포외기질 (ECM) 재형성과 관련된 유전자의 발현이 증가하였다. 게다가, 세포간 상호작용 분석에서 낮은 TIL 수준의 그룹에 비해 높은 TIL 수준의 HR+ 유방암에서 단핵구 및 대식세포와 T 세포 사이의 상호작용에서 증가된 SPP1 신호전달을 보여주었다. HR+ 유방암의 공간전사체 분석에서 우리는 낮은 TIL 수준의 데이터에 비해 높은 TIL 수준의 데이터에서 단핵구 및 대식세포와 CD8+ T 세포 및 CD4+ T 세포의 근접성을 강조하였다. 종합적으로, 우리는 높은 TIL 수준의 HR+ 유방암의 종양미세환경 내 T 세포에 영향을 미치는 SPP1을 발현하는 단핵구 및 대식세포의 새로운 역할을 발견하였다. 이러한 발견은 높은 TIL 수준과 연관된 HR+ 유방암의 나쁜 예후를 설명할 수 있으며, 이는 SPP1+ 대식세포가 그들의 예후를 개선하기 위한 잠재적인 대상이 될 수 있음을 시사한다.

주제어 : 유방암, 호르몬 수용체 (HR), 종양침윤림프구, 종양관련대식세포, 분비 인단백질 1 (SPP1)